

# MINERAL CHARACTERIZATION IN GEOSYNTHETIC CLAY LINERS USING MICRO-XRAY DIFFRACTION

K. Lange, R.K Rowe and H. Jamieson

*GeoEngineering Centre at Queen's - RMC, Queen's University, Kingston, ON, Canada*

R.L. Flemming

*Department of Earth Sciences, University of Western Ontario, London, ON, Canada*



## ABSTRACT

Until recently, characterization of geosynthetic clay liner (GCL) bentonite had been limited to conventional powder X-ray diffraction (XRD). In this case, clays minerals were determined based on homogenized bulk samples and this routinely involved physical or chemical separation methods which can destroy or contaminate the sample. In addition, the minor minerals that comprise less than approximately five percent of the sample have not been accessible to identification by XRD. Knowledge of the structure and composition of the bentonite on the micron scale is essential for delineating the retention mechanisms of introduced metals, such as the formation of new mineral phases. With this aim, the minerals comprising the bentonite in GCLs were characterized using a combination of micro XRD data and elemental information from XRF (X-ray fluorescence) maps. The two dimensional image from the GADDS detector has been particularly advantageous in differentiating between the microcrystalline clay, which appeared as homogeneous Debye rings, and the 'spotty' or 'grainy' appearance of primary, more-coarsely- crystalline, accessory minerals. Thus, examination by microXRD did not require physical separation of the sample. Using this technique, smaller quantities of clay minerals such as nontronite (smectite) and biotite (mica) were identified to be present in addition to the bentonite, and polymorphs of quartz and calcite were distinguished. Using this information and the above advanced analytical techniques, the identification of metal attachment sites and preferential metal sorption sites can be made much more reliably.

## RÉSUMÉ

Jusqu'à récemment, la caractérisation de la bentonite des géosynthétiques bentonitiques (GSB) était conventionnellement limitée à la diffraction des rayons X (XRD) sur la poudre de bentonite. Dans ce cas, les minéraux argileux sont déterminés à partir d'échantillons bruts homogénéisés et ceci implique des méthodes de séparation physiques ou chimiques de routine qui peuvent détruire ou contaminer l'échantillon. De plus, la caractérisation des minéraux minoritaires qui représentent moins de cinq pour cent environ de l'échantillon n'étaient pas réalisable par XRD. La connaissance de la structure et de la composition de la bentonite à l'échelle du micron est essentielle pour isoler les mécanismes de rétention de métaux introduits, tels que la formation de nouvelles phases minérales. C'est dans cet objectif que les minéraux contenant la bentonite dans des GSB ont été caractérisés en utilisant une combinaison de données de micro-XRD et des informations sur les éléments acquises par XRF (fluorescence des rayons X). L'image à deux dimensions du détecteur GADDS a été particulièrement avantageuse pour différencier l'argile microcristalline, qui est apparue sous la forme d'anneaux de Debye homogènes, et l'apparence « à pois » ou « granulaire » des minéraux cristallins et accessoires primaires plus grossiers. Ainsi, l'examen par microXRD n'a pas exigé la séparation physique de l'échantillon. Lors de l'utilisation de cette technique, de plus petites quantités de minéraux d'argile tels que la nontronite (smectite) et la biotite (mica) ont été identifiées en plus de la bentonite, et les polymorphes de quartz et de calcite ont été repérés. L'utilisation de cette information et des techniques analytiques présentées ci-dessus permet une identification plus fiable, de sites de fixation des métaux ainsi que des sites préférentiels de sorption des métaux..

## 1 INTRODUCTION

The increased use of geosynthetic clay liners (GCLs) in waste barrier systems has prompted many studies to examine their engineering behaviour (hydraulic conductivity, swell index, change in cation exchange capacity) in the presence of leachates (e.g. Kolstad et al. 2004, Rowe et al., 2005). Researchers continue to examine their ability to attenuate various contaminants, including metals, which are attributed to the high pH, surface area, and cation exchange capacity of the

sodium-bentonite used in many GCLs (e.g. Rowe et al. 2005; Lange et al. 2007).

In metals-contaminated soils and sediments, attention has recently been given to microanalytical techniques (Bertsch and Seaman 1999; Roberts et al. 2002; Scheidegger et al. 1997, Walker et al, 2005.). Such studies using advanced spectroscopic and microscopic techniques such as  $\mu$ -synchrotron based X-ray fluorescence spectroscopy ( $\mu$ -SXRF), micro X-ray diffraction ( $\mu$ XRD) and X-ray absorption fine structure

spectroscopy (XAFS), have shown that the formation of surface precipitates are important in metal sorption (e.g. Isaure et al. 2005; Scheidegger et al. 1997). Effective pollution prevention using soil material, especially for metal containment, also requires an understanding of metal mobility at the scale of individual mineral grains, but few data are available on specific applications to barrier materials (Daniels et al. 2004). Familiarity of the structure and composition of the soil material at the micron scale is necessary for delineating the retention mechanisms of introduced metals, such as the formation of new mineral phases.

Characterization of similar geosynthetic clay liner (GCL) bentonite has been conducted using conventional powder X-ray diffraction (XRD) (Rowe et al. 2000). Determination of clay minerals are typically determined based on homogenized bulk samples, and routinely involves some physical and/or chemical separation methods (e.g. Henderson et al. 1971) which can lead to sample contamination. In addition, details of the secondary minerals that comprised less than five percent of the sample were not accessible to identification by XRD. Advanced microanalytical techniques give the possibility for non-destructive, in situ investigation of the sample and open unique possibilities in the study of barrier materials that compliment bulk analysis.

Flemming et al. (2005) examined arsenic-rich secondary phases in mine waste by a combination of  $\mu$ XRD and electron probe micro-analysis (EPMA). They identified two texturally distinct occurrences of scorodite in specific areas of polished thin sections. The fine-grained polycrystalline scorodite material was easily discernable from the relatively coarse-grained primary materials using the two dimensional (2D) image from the General Area Diffraction Detector system (GADDS detector). In the current study, the mineralogical and elemental composition of the bentonite in GCLs has been examined by combining  $\mu$ XRD methods, similar to that used by Flemming et al. (2005) with synchrotron-generated  $\mu$ -XRF elemental mapping. A comprehensive understanding of the GCL "starting material" is critical to any studies aimed at the, the identification of metal attachment sites and preferential metal sorption sites of GCLs exposed to metal-contaminated leachates.

### 1.1 GCL Bentonite

Previous work by Rowe et al. 2000 found the GCL bentonite mineralogy to consist of 91 percent smectite (sodium-montmorillonite), 5 percent quartz, 3 percent feldspar and 1 percent carbonate. They also reported the principle ions in the pore water (when bentonite is at the liquid limit) and their concentrations:  $\text{Na}^+$  (12.13 meq/L),  $\text{Ca}^{2+}$  (1.16 meq/L),  $\text{Mg}^{2+}$  (0.48 meq/L) and  $\text{K}^+$  (0.20 meq/L).

Smectites, also known as 'expanding clays', are typically divided into two major families: 'di' and 'tri' octahedral. These minerals can easily accept ions and polar molecules in the interlayer position thus changing the overall cell dimension in the basal direction (Velde 1985). Therefore the minerals can be easily identified by

interaction with water or ethylene glycol that changes the basal spacing (e.g. at room temperature, montmorillonite expands from 14.7Å up to 17.7Å upon ethylene glycol saturation).

Montmorillonite, the primary mineral in the GCL bentonite, is a dioctahedral smectite clay where a divalent ion substitutes for a trivalent ion in its' octahedral site (Yong, 2001). Another substitution is that of beidellite and nontronite where a trivalent ion replaces the quadrivalent silicon (Velde 1985).

## 2 METHOD: MICROANALYTICAL TECHNIQUES

The GCL tested in this study was a BENTOFIX™ NWL GCL distributed by Terrafix Geosynthetics Inc. The GCL consisted of a nonwoven carrier geotextile, a layer of granular Wyoming sodium bentonite and a nonwoven cover geotextile needlepunched together with the fibers thermally treated on the carrier geotextile. Bentonite was removed from the GCL, and grounded with a mortar and pestle. The clay was then mixed with epoxy before being mounted on a glass slide and doubly polished (both sides) to a thickness of 30-50 microns. The thin sections were examined and documented using a petrographic microscope in both reflected and transmitted light.

### 2.1 $\mu$ -Synchrotron based X-ray fluorescence spectroscopy

Synchrotron-based hard x-ray microprobes are specifically advantageous to the study of trace metals due to higher spatial resolution (<10  $\mu\text{m}$ ) and higher analytical sensitivity (femtogram detection) than is possible using normal laboratory-based instruments, and does not require physical separation of the sample. The in situ  $\mu$ -synchrotron based X-ray fluorescence spectroscopy ( $\mu$ -SXRF) analysis occurred at the Department of Energy's National Synchrotron Light Source (NSLS), at Brookhaven National Laboratory on the X26A beamline. The  $\mu$ XRF mapping technique was used to show the distributions of 8 elements (simultaneously): Cr, K, Ca, Mn, Zn, As, Ni, Cu. The fluorescent and scattered radiation emerging from the sample is detected by a Radiant Vortex-EX Silicon Drift detector. Detailed maps ranging from 0.1  $\text{mm}^2$  to 3  $\text{mm}^2$  with as low as 0.01 mm resolution were recorded by scanning in the focused beam (5 microns) at 17.2 keV (high energy). The  $\mu$ -SXRF maps and images were used to select targets for  $\mu$ XRD. Special care was taken to choose areas that minimized overlapping textures.

### 2.2 Micro X-ray diffraction ( $\mu$ XRD)

$\mu$ XRD data on targeted grains were collected with the Bruker D8 Discover diffractometer at the University of Western Ontario, operating with Cu K $\alpha$  radiation ( $\lambda = 1.5418 \text{ \AA}$ ) at 40 kV and 40 mA and a 500  $\mu\text{m}$  spot size. A full description of this apparatus is available in Flemming et al. 2005. Briefly, the theta-theta ( $\theta$ - $\theta$ ) geometry allows analysis of samples in various forms such as loose grains

as the sample is stationary in the horizontal position, while the X-ray tube and the detector both move simultaneously over the angular range  $\theta$ . The omega scan function was also used to increase the number of reflections that satisfy the Bragg diffraction thus enhancing the capability to deal with a wide range of samples, from polycrystalline to single crystals. The two dimensional (2D) image GADDS is key in differentiating between the microcrystalline clay and coarser crystallite mineral phases by evaluating the continuity and broadening of the Debye-Scherrer rings. XRD patterns at  $2\theta$  from 10 to 80 were recorded, each frame taking 960 seconds (two frames per target).

Previous work had shown that synchrotron-based  $\mu$ XRD on thin sections is possible if the sample is 'lifted' from the glass slide using acetone (Walker et al, 2005). However, in the case of the clay-rich material, preservation of the sample integrity during 'lifting' was unsuccessful. The nonsynchrotron-based  $\mu$ XRD does not require removal from glass, and also allows for good optical control of the sample.

### 3 RESULTS

In thin section, the epoxy-impregnated GCL bentonite, varied in colour from orange-brown to grey-black). Individual accessory minerals and agglomerated clay particles were visible (Figure 1a).

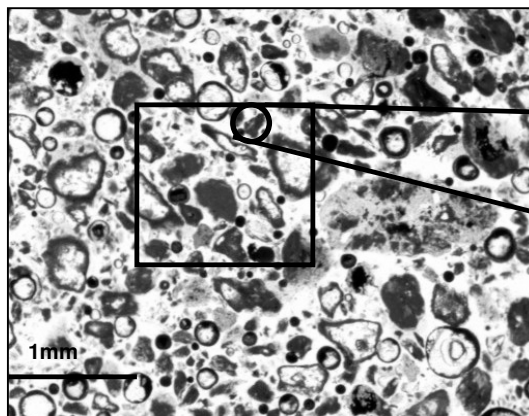


Figure 1(a). Polished epoxy thin section of GCL bentonite, transmitted light. Boxed area indicates perimeter for micro-XRF mapping. Circle shows targeted area '4'.

Targeted areas of the thin sections were selected that best (visually) represented the overall sample. Figure 2 shows the corresponding synchrotron-based  $\mu$ -XRF area map of the area in Figure 1a), for 6 elements: Fe, K, Ca, Mn, As and Ti. The dimensions of the map are 1.4 by 1.5 mm in the x and y respectively, with 0.05 mm discretized spacing. Elemental maps provide valuable information even without  $\mu$ XRD. From the two high Ca areas seen in Figure 2, one is mirrored by a high Mn area, indicating that these minerals may not be the same. The Fe rich area on the top right of the map ( $x=1.35, y=1.21$ ), mirrors an As rich area. Given this information and the reddish color, this is likely an iron oxide. Similarly, a very high spot of both Ti and Fe occur on the top middle of the map; titanium oxides such as ilmenite are common in nature. Small amounts of K are scattered throughout the map, likely from traces of K-feldspar. Multiple overlaying element plots and correlation plots (not shown here) also provide relative abundances and help to confirm associations. The maps show almost no presence of Ni, Cr, and Cu, and only minor occurrences of Zn.

The 2d  $\mu$ -xrd patterns for the selected grain (circle on Figure 1(b)) are displayed in Figure 3; this was a common pattern seen in the data collected from this samples. The corresponding 1d integration is shown in Figure 4. The two dimensional image from the GADDS detector shows how the microcrystalline montmorillonite clay appears as homogeneous Debye rings of constant intensity. The primary, more-coarsely crystalline accessory minerals appear as spots or have a grainy appearance.

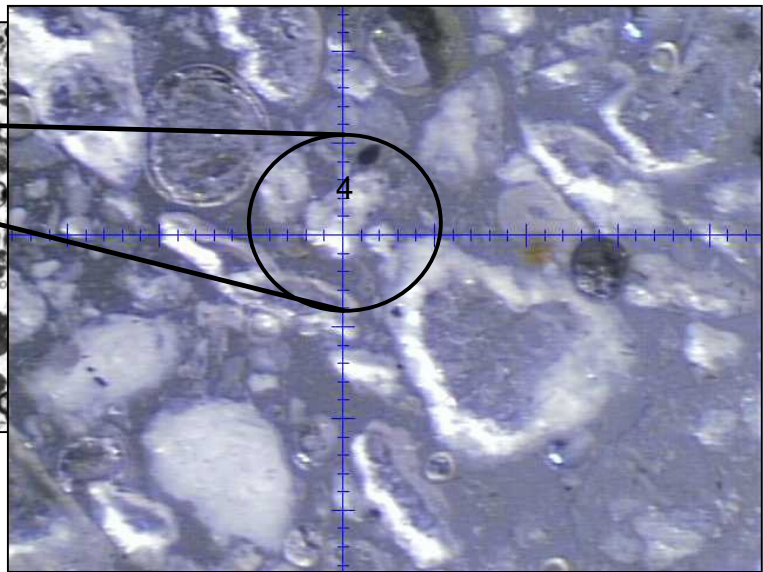


Figure 1(b). Photo taken from camera positioned within micro-diffractometer setup, reflected light. Circle shows targeted area '4'.

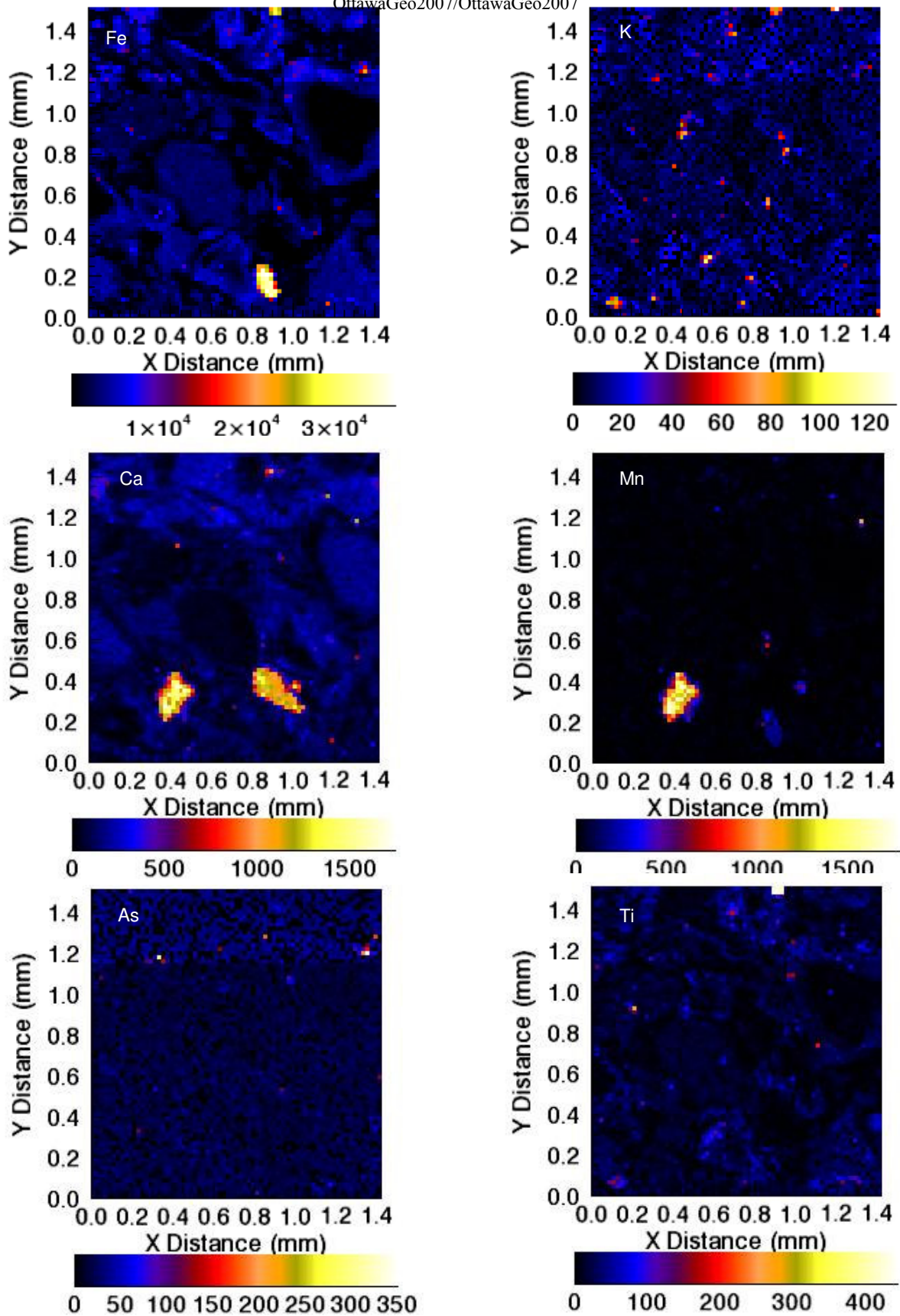


Figure 2. Synchrotron-based micro-XRF area map of the square in Figure 1(a), for 6 elements: Fe, K, Ca, Mn, As and Ti. Dimensions of the map: 1.4 by 1.5 mm in the x and y respectively, with 0.05 mm discretized spacing.

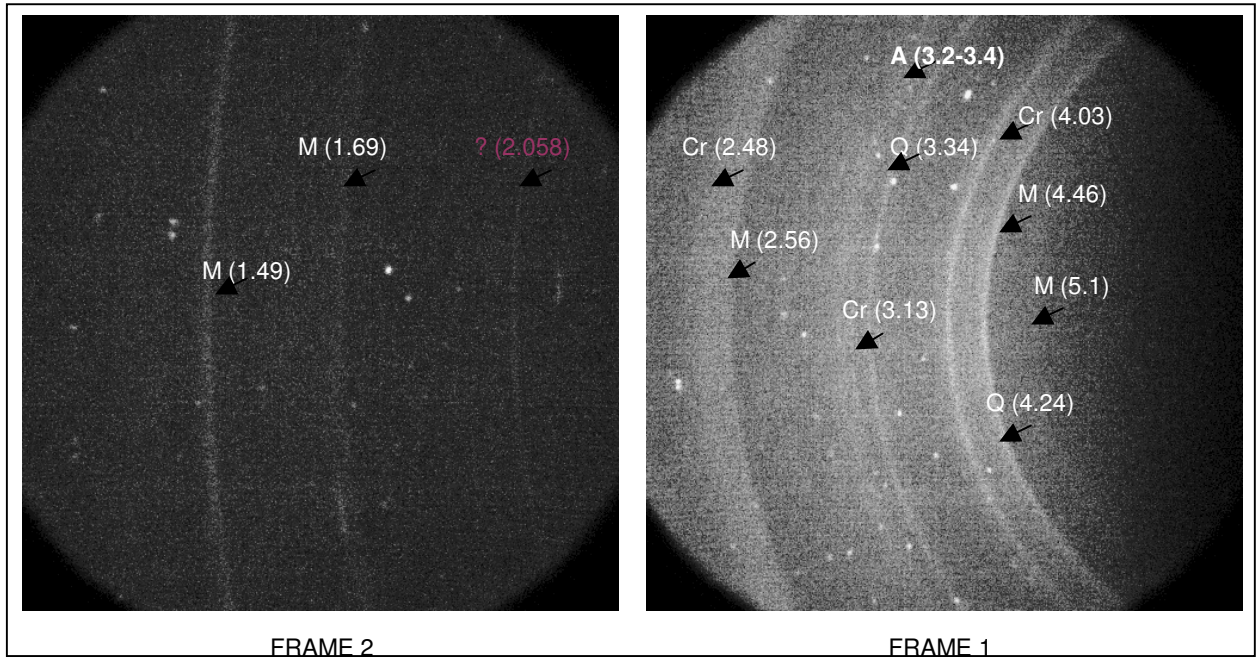


Figure 3. GADDS image of targeted area '4'. Frame 1: theta1=6.0, theta2=17.0. (960 seconds) Frame 2: theta1=16, theta2=40.

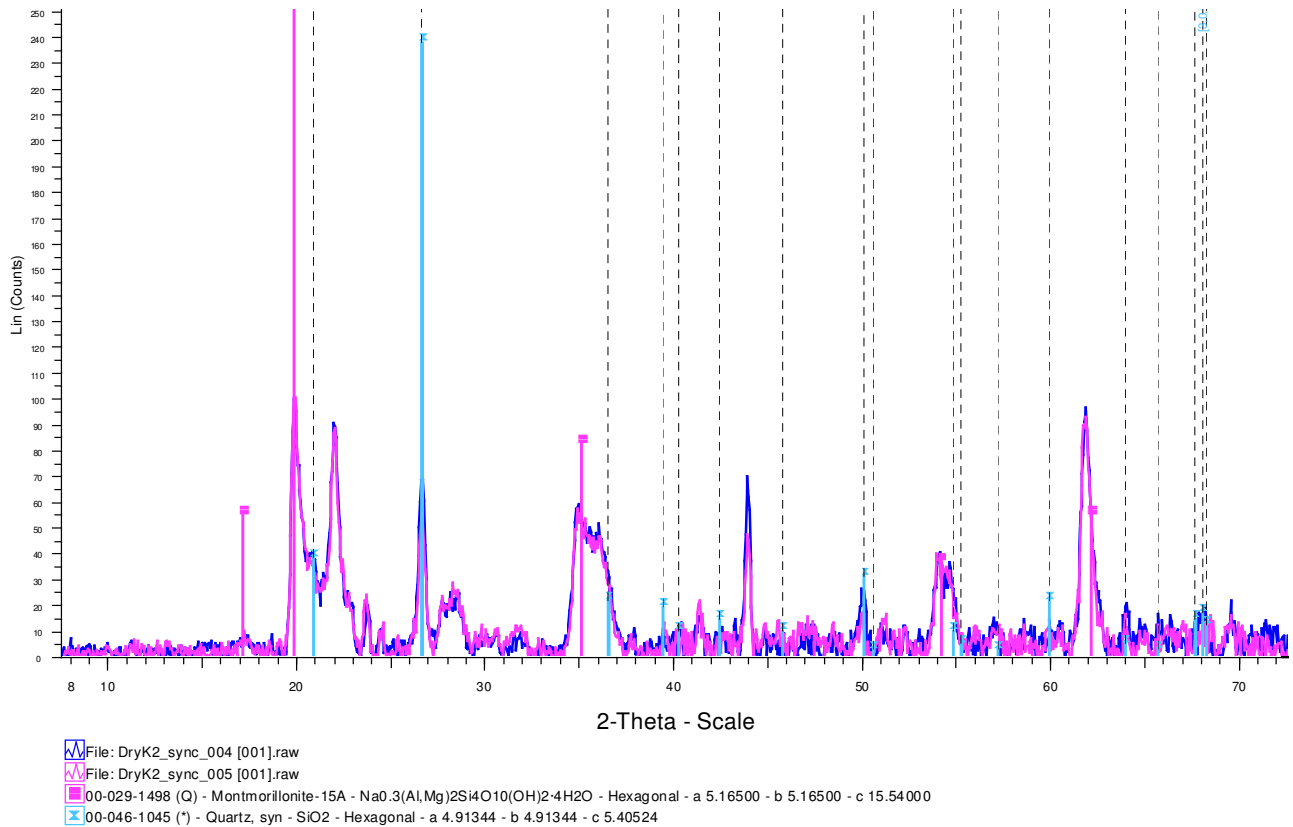


Figure 4. Integration of 2D GADDS image. 1D Intensity versus 2-Theta plot for target '4'.

An agglomeration of dots appearing after the second quartz ring ( $d=3.34$ ) correspond to anorthite (Ca-feldspar). Microcrystalline quartz appeared in all samples tested, producing very thin lines, mostly appearing as a series of connected tiny dots, with some larger point reflections. In one case, a region of very high Fe, had a diffraction pattern corresponding to quartz, suggesting that the detrital quartz was coated with Fe. Cristobalite produced a series of thick continuous lines (e.g.  $d=4.03, 3.13, 2.48$ ). Cristobalite and smectite have been reported to form very fine intergrown aggregates in some bentonite samples included from the Wyoming region (Güven and Grim 1972). The authigenic origin of cristobalite related to montmorillonite and quartz is discussed by Henderson et al. (1971). Smaller quantities of the clay minerals showing similar rings were identified as nontronite (smectite), and biotite (mica). Point diffraction spots were identified as: albite, anorthite, gypsum, polymorphs of calcite, and titanium and red iron oxides (hematite).

The identification and characterization of the bentonite by  $\mu$ -XRF mapping and  $\mu$ -XRD provided a 'baseline' reference for the purpose of investigating metal retention in future GCL barrier scenarios. Knowledge of secondary minerals could be beneficial for identifying newly precipitated phases. Also these secondary minerals may consist of highly sorbent materials such as iron oxides that have been known to play a major role in sequestering certain metals.

#### 4 CONCLUSION

Novel analytical methods such as  $\mu$ XRD and synchrotron-based x-ray fluorescence techniques provide the possibility of non-destructive, in situ investigation of various soil characteristics with micro spatial resolution. The results herein demonstrated the importance of combining such advanced techniques to accurately characterise the distribution of key elements and minerals in bentonite, as each technique has limitations. In this case analyses were made using (1)  $\mu$ -XRF spatial data of 8 elements on a micron scale, (2) microscopic imaging of the specimen (3) 2-D  $\mu$ XRD (GADDS) representation (4) 1-D  $\mu$ XRD representation.

To our knowledge this is the first study that analyzes GCLs in such a way, and the results should prove valuable in metal sequestering analysis. In particular, distinguishing accessory crystalline phases present in the "starting material" bentonite from those formed as a result of interaction with metal-bearing leachates is critical, as the development of metal-attenuating crystalline phases can have a significant long-term impact on metal mobility.

#### ACKNOWLEDGEMENTS

We would like to acknowledge Mr. K. Von Mauberge and B. Herlin from Terrafix for their valuable help and discussion involving GCLs. We would also like to acknowledge Antonio Lanzirrotti for his help and

guidance at beamline X26A (NSLS); and the micro-diffraction laboratory/staff at the University of Western Ontario. This work was funded by Terrafix, The Ontario Centre of Excellence (OCE), and NSERC discovery grants and student scholarship. Synchrotron work was performed at Beamline X26A, National Synchrotron Light Source (NSLS), Brookhaven National Laboratory. X26A is supported by the Department of Energy (DOE) - Geosciences (DE-FG02-92ER14244 to The University of Chicago - CARS).

#### REFERENCES

- Bertsch, P.M., Seaman, J.C. (1999) Characterization of complex mineral assemblages: Implications for contaminant transport and environmental remediation. *Proc. Natl. Acad. Sci. USA Colloquium Paper*, Vol. 96: 3350–3357.
- Daniels, J.L., Inyang, H.I., Chien, C. (2004) Verification of Contaminant Sorption by Soil-bentonite barrier materials using scanning electron microscopy/energy dispersive x-ray spectrometry, *Journal of environmental engineering ASCE*, 130(8) : 910-917.
- Flemming, R.L., Salzsauler, K.A. Sherriff, B.L. and Sidenko, N.V. (2005) Identification of scorodite in fine-grained, high-sulfide, arsenopyrite mine-waste using micro x-ray diffraction, *The Canadian Mineralogist*, 43 : 1243-1254.
- Gnanendran, C.T., and Selvadurai, A.P.S. 2001. Strain measurement and interpretation of stabilizing force in geogrid reinforcement, *Geotextiles and Geomembranes* 19: 177-194
- Güven, N. and Grim, R.E. (1972) X-ray diffraction and electron optical studies on smectite and a-cristobalite associations, *Clays and Clay Minerals*, 20: 89-92. Pergamon Press, Great Britain
- Henderson, J.H., Jackson, M.L., Syers, J.K. (1971) Cristobalite Authigenic Origin in relation to montmorillonite and quartz origin in bentonites, *Clays and Clay Minerals*, 19:229-238.
- Ingold, T.S. and Miller, K.S. 1983. Drained axisymmetric loading of reinforced clay, *Journal of Geotechnical Engineering*, ASCE, 109: 883-898.
- Kolstad, D., Benson, C.H., and Edil, T.B. (2004) Hydraulic Conductivity and Swell of Nonprehydrated GCLs Permeated With Multispecies inorganic solutions, *Journal of Geotechnical and Geoenvironmental Engineering*, 130(12):1236-1249.
- Lange, K., Rowe, R.K., Jamieson, H.J. (2007) Metal retention in geosynthetic clay liners following permeation by different mining solutions, *Geosynthetics International*, 14(3):178-187.
- Roberts, D.R., Scheinost, A.C. Sparks, D.L. (2002) Zinc Speciation in a Smelter-Contaminated Soil Profile Using Bulk and Microspectroscopic Techniques, *Environ. Sci. Technol.* 36: 1742-1750.
- Rowe, K.R. Mukunoki, T. and Sangam, H.P. (2005) BTEX Diffusion and Sorption for a Geosynthetic Clay Liner at two temperatures, *Journal of geotechnical and geoenvironmental engineering*, ASCE, 131 (10): 1211-1221.

- Rowe, R.K., Lake, C.B., and Petrov, R.J. (2000) Apparatus and Procedures for Assessing Inorganic Diffusion Coefficients for Geosynthetic Clay Liners, *Geotechnical Testing Journal*, 23: 206-214
- Scheidegger, A.M., Lamble, G.M., and Sparks, D.L. (1997) Spectroscopic Evidence for the Formation of Mixed-Cation Hydroxide Phases upon Metal Sorption on Clays and Aluminum Oxides, *Journal of Colloid and Interface Science* 186:118-128
- Velde, B. (1985) Clay Minerals – A Physico-Chemical Explanation of their occurrence. *Developments in Sedimentology*. Elsevier. N.427 pp.
- Walker, S.W., Jamieson, H.E., Lanzirotti, A., Andrade, C.F. 2005 Determining arsenic speciation in iron oxides derived from a gold-roasting operation: Application of synchrotron micro-XRD and micro-XANES at the grain scale. *Canadian Mineralogist* 43, 1205-1224.
- Yong, R. N. 2001. Geo-environmental Engineering, 1<sup>st</sup> Edition, CRC Press LLC, USA.